



Bioactive nano-selenium antagonizes cobalt nanoparticle-mediated oxidative stress via the Keap1-Nrf2-ARE signaling pathway

Siqi Wang · Chen Wang · Weinan Zhang · Wentao Fan · Fan Liu · Yake Liu

Received: 6 September 2021 / Accepted: 30 December 2021 / Published online: 13 January 2022
© The Author(s) 2022

Abstract At present, no effective treatment exists for the clinical toxicity of cobalt nanoparticles (CoNPs, 30 nm) after metal-on-metal (MOM) artificial joint replacement. As such, a better understanding of the CoNPs-toxicity mechanism is necessary and urgent for the development of effective and safe detoxification drugs. Our purpose was to explore the role of bioactive nano-selenium (BNS, >97%) in antagonizing the toxicity of CoNPs and its mechanism through the Keap1-Nrf2-ARE signaling pathway. To examine BNS detoxification, we exposed HUVEC cells to CoNPs and BNS for 24 h, before measuring cell activity, reactive oxygen species (ROS), the GSH level, inflammatory factors, and KNA signaling pathway-related transcript and protein expression. CoNPs stimulate intracellular inflammation and ROS production to bring about significant downregulation of cellular activity and the GSH level. Conversely, BNS reduces ROS generation and suppresses inflammatory factors within cells to reduce CoNPs-mediated

cytotoxicity, possibly via the KNA signaling pathway. Based on our results, BNS antagonizes CoNPs toxic effects by suppressing ROS production through the KNA pathway. Our research provides new insight into the clinical treatment of CoNPs toxicity and explores the potential of BNS in detoxification therapy. Trial registration: no human participant.

Keywords Cobalt · Nano-selenium · Keap1-Nrf2-ARE · ROS · Nanobiomedicine · Nanoparticle toxicity

Introduction

Artificial joint replacement is a prosthetic surgery whereby the diseased articular cartilage and the bone are replaced with an artificial implant. It has been widely used as an effective treatment for end-stage joint disease (Li and Glassman 2019). Among the large number of prosthetics available, the metal-on-metal (MOM) artificial joints are the most popular, due to its remarkably high strength and wear resistance (Learmonth et al. 2007). However, due to its high cobalt-chromium alloy content, MOM often releases a large number of cobalt nano particles (CoNPs) into the human body, due to wear (or physical) and chemical factors (Saikko 2019). Multiple studies have reported CoNPs to be highly toxic. In particular, they have been shown to stimulate intracellular oxidative stress,

Siqi Wang and Chen Wang contributed equally to the article.

S. Wang · C. Wang · W. Zhang · W. Fan · F. Liu (✉) · Y. Liu (✉)

Department of Orthopaedics, Affiliated Hospital of Nantong University, 20 Xisi Road, Nantong 226001, Jiangsu Province, China
e-mail: liufan19515@126.com

Y. Liu
e-mail: yakeliu@sina.com

DNA damage, tissue inflammatory response, and cyto- and genotoxicity(Liu et al. 2015; Zheng et al. 2019). Clinically, the CoNPs side effects present as cobalt cardiomyopathy(Packer 2016), osteolysis around the prosthesis(Preedy et al. 2015), genetic toxicity(Kirkland et al. 2015), hearing and vestibular dysfunction(Leyssens et al. 2020), blood system diseases like lupus erythematosus and white blood cell abnormalities(Reich et al. 2019), malignant tumors, inflammatory pseudotumors, and so on. In the skeletal system, for instance, CoNPs affect the growth and differentiation of osteoblasts, and indirectly upregulate the dissolution and absorption of bone by osteoclasts, thereby accelerating osteolysis around the prosthesis(Perni et al. 2018). Based on ample detrimental evidence, the International Agency for Research on Cancer (IARC) listed CoNPs as potentially carcinogenic to humans and graded it as 2B. Our previous research has also confirmed the toxicity of CoNPs on a variety of cells. However, the underlying mechanism still remains to be investigated.

CoNPs are minute particles, averaging a diameter of 30 nm. They are mostly released from the interface wear of artificial joints. Several factors affect the wear of MOM, including implant type, implant position, swing phase load, fluid chemistry, wear process, and isolation technology(Madl et al. 2015). Moreover, with stress bending, scratching, and impact, the surface oxide layer of MOM tends to degrade, thereby releasing CoNPs. In addition, both crevice and galvanic corrosions at the prosthetic joint components, under acidic conditions, further accelerate the release of CoNPs(Han and Liu 2017). Moreover, CoNPs that are not absorbed by the bone can be freely available to multiple organ systems and can exist in the forms of particles and corrosion debris, metal-protein complexes, or free metal ions(Polyzois et al. 2012). As a result, CoNPs presence can be detected in multiple organ systems like the liver, kidney, pancreas, myocardium, lung, testis, ovary, and so on. Based on published literature, only a small amount of CoNPs can be eliminated from the body through the kidneys(Wan et al. 2017; Liu et al. 2016; Rasool et al. 2020).

Reactive oxidative stress (ROS) plays a major role in the toxicity of CoNPs. Once CoNPs enter a cell, they stimulate the production of excessive reactive oxygen species through the Fenton reaction, which in turn, oxidizes cell biomolecules, including DNA, causing DNA strand breakage, and induce a

series of other oxidative damage(Zorov et al. 2014). One of the signaling pathways affected by CoNPs is the Keap1-Nrf2-ARE (KNA) antioxidant signaling pathway(Zhang et al. 2010). ROS is known to activate the KNA pathway, which prompts the activation of a large number of downstream antioxidant enzymes, such as heme oxygenase-1 (HO-1), human quinone peroxidase-1 (NQO-1), and so on(Kovac et al. 2015). This is likely the cell's defense mechanism against the toxicity of CoNPs. As a result, in this study, we suspected the artificial activation of the KNA pathway to be an effective therapy for CoNPs toxicity.

Bioactive nano-selenium (BNS) is a known antioxidant that minimizes oxidative stress in cells(Alkudhayri et al. 2018; Vera et al. 2018; Miroliac et al. 2011). It is also responsible for generating strong anti-oxidant selenoproteins in the form of selenocysteine, such as GSH. Given its strong antioxidant property, we suspected that BNS mediates its actions via the KNA pathway, and can be used to antagonize CoNPs toxicity(Xiao et al. 2019; Song et al. 2017). To test this hypothesis, we evaluated oxidative stress and the underlying mechanism in human umbilical vein endothelial cells (HUVECs), exposed to BNS and/or CoNPs. Based on our results, we have confirmed our hypothesis that BNS protects cells from CoNPs-mediated oxidative stress through the activation of the KNA pathway.

Materials and methods

Reagents and chemicals

Culture media and solutions like Roswell Park Memorial Institute (RPMI-1640), fetal bovine serum (FBS), penicillin/streptomycin, Trypsin-EDTA, and Phosphate-Buffered Saline (PBS) were purchased from Gibco (Life Technologies, Paisley, UK). Cobalt chloride (Co^{2+}) and CoNPs (30 nm, 99.9%) were purchased from Shanghai Chaowei Nano Technology Co., Ltd. (Shanghai, China), and BNS (20 mg/ml, >97%) was sponsored by the Tianjin Orthopaedic Research Institute (Tianjin, China). Ten percent of polyacrylamide gel premix (NCM FastPAGE), RIPA Lysis Buffer, and NcmECL Ultra were purchased from New Cell & Molecular Biotech Co., Ltd. (Suzhou, China). Lastly, all antibodies were purchased from Abcam (Cambridge, UK).

Cell culture

Human umbilical vein endothelial cells (HUVECs) were purchased from the China Center for Type Culture Collection (CCTCC). The cells were cultured in RPMI-1640 media supplemented with 10% FBS, along with penicillin (100U/ml) and streptomycin (100 µg/ml). The medium was replaced daily. All cells were grown in a humidified incubator at 37°C containing 5% CO₂. During experimentation, the HUVECs were exposed to specific concentrations of CoNPs (400 µmol/l) for 24, 48, and 72 h to induce CoNPs-mediated toxicity. To test the protective effects of BNS, HUVECs cells were exposed to CoNPs (400 µmol/l) and BNS for 24 h before examining cell viability, ROS production, inflammatory factors, and related protein expression.

Preparation of Co²⁺, CoNPs, and BNS

Co²⁺ was suspended in ultrapure water at an initial concentration of 1 mM, using a 0.22-µm filter to sterilize and diluted in complete culture medium accordingly to achieve the required concentrations. CoNPs were weighed, according to the tested dosages (400 µmol/l), sterilized in a high-pressure steam cooker for 4 h, then suspended in ultrapure water at a concentration of 40 mmol/l, shaken, and mixed in an ultrasonic oscillator for 15 min, before diluting with basic medium (RPMI-1640) to the concentrations used in the experiments. The prepared CoNPs suspensions were stored in a refrigerator at -20 °C until experimentation. BNS (20 mg/ml), obtained from the Tianjin Institute of Orthopaedics, was irradiated and sterilized under ultraviolet light for 2 h, before diluting to 200 µg/ml with basal media for subsequent experiments. The diluted BNS was stored at -20 °C.

Characterization of CoNPs

The methods of the CoNPs characterization were described in our previous work³⁴. The size, microstructure, and elemental composition of CoNPs were assessed by high-resolution scanning electron microscopy (Hitachi 550 ultrahigh resolution SEM), transmission electron microscopy (TEM; JEM-2100F, Japan) and X-ray diffraction (XRD). In brief, CoNPs were suspended in DMEM supplemented with 5% FBS at a concentration of 1 mg/mL

(pH 7.2–7.4), and then the sample was sonicated by using a sonicator bath until a homogeneous suspension formed. A drop of aqueous CoNPs suspension was placed onto a carbon-coated copper grid (300 mesh) and dried in air to obtain SEM and TEM images. XRD was employed for elemental analysis. Dynamic laser light scattering (DLS) measurements were used to determine the hydrodynamic diameter and size distribution of Co nanoparticles in the cell culture medium.

Cell viability assay

The Cell Counting Kit-8 (CCK-8, Beyotime Company, Jiangsu, China) was used to analyze CoNPs toxicity and BNS detoxification in HUVEC cells. The cells were seeded, at a density of 1×10^4 cells/well in a 96-well plate, using RPMI-1640 with 10% FBS and penicillin (100U/ml) and streptomycin (100 µg/ml) and placed in a humidified incubator at 37 °C, 5% CO₂ for 24 h. Cells were exposed to CoNPs (0, 25, 50, 100, 200, 400, 600, or 800 µmol/l) for 24 h to explore the IC₅₀ value. Next, the original medium was replaced with media containing a varying concentration of CoNPs or/and BNS. After 24 h, 48 h, and 72 h of incubation with CoNPs or/and BNS, 100 µl of CCK-8 solution, diluted to 10% concentration with basic medium (RPMI-1640), was added to the cells. After 2 more hours of incubation, the absorbance at 450 nm was measured using a microplate reader (Japan Intermed, Tokyo, Japan). Lastly, the relative survival rates of cells, exposed to CoNPs and BNS, for 24 h, 48 h, and 72 h were recorded.

Cytokine detection

Cells were plated at a density of 1×10^5 cells/well in six-well plates and incubated for 24 h at 37°C, 5% CO₂. Next, CoNPs (400 µmol/l) was administered to the cells, with or without the treatment of BNS (50 µg/ml), for 24 h. Following this, the cell media was analyzed for the presence of secreted inflammatory factors IL-1β, IL-6, and TNF-α, using the ELISA kit (R&D Systems, Minneapolis, MN), following manufacturer's guidelines. Each experiment was repeated 3 times.

Quantification of intracellular ROS

A ROS detection kit (Beyotime Company, Jiangsu, China) and fluorescence imaging were employed to analyze intracellular ROS production in cells exposed to CoNPs and/or BNS. In short, cells were plated at a density of 1×10^5 cells/well in six-well plates and incubated for 24 h at 37 °C, 5% CO₂. Then, the original medium was replaced with medium containing CoNPs (400 μmol/l) and/or BNS (50 μg/ml) for 24 h. Next, the cells were incubated with the DCFH-DA from the ROS detection kit for 20 min at 37 °C, 5% CO₂ before PBS-washing the cells 3 times, and observing them under a microscope. The cell morphology and number were recorded under bright field before quantifying the intracellular ROS generation under a fluorescence microscope. The relative values are expressed as a percentage of the fluorescence intensity, as compared to the control.

GSH measurement

GSH was determined in the cells with CoNPs (400 μmol/l) and/or BNS (50 μg/ml) for 24 h. The blank group, positive control group (CoNPs, 400 μmol/l), and a negative control group (BNS, 50 μg/ml) were also established at the same time. After the exposure, the cells were washed with PBS twice, scraped off, suspended in PBS, and centrifuged at $1000 \times g$. The cell pellet was then homogenized in 5% 5-sulfosalicylic acid. Next, the suspension was lysed by freezing and thawing twice after 5 min centrifuged at $10,000 \times g$ for 10 min. Intracellular total GSH concentrations were measured according to the supplier's protocol.

Protein analysis using western blot

The cells were plated at a density of 4×10^5 cells/well in six-well plates and incubated for 24 h at 37 °C and 5% CO₂. In order to collect all the proteins in the system to ensure the accuracy of the experiment, we collected the cells, cell supernatant, and washed PBS. The cells were then exposed to CoNPs (400 μmol/l) and BNS (50 μg/ml) for 24 h, and the cells media was collected. The remaining cells were once washed with PBS, and the PBS wash was collected. Next, the cells were lysed using RIPA protein lysis buffer (50 mM Tris-HCl (pH 7.4), 150 mM NaCl, 1% NP-40, 0.1%

SDS) on ice for 30 min, and the resulting cell solution was mixed with the previously stored media and PBS wash. The combined solution was then centrifuged at $12,000 \times g$ for 15 min, and the supernatants were recovered. The protein concentration was measured using a spectrophotometer and the reconstituted protein was stored at -80°C until western blot analysis. The western blot analysis was conducted with NCM FastPAGE separating gel and concentrated gel and the resulting membrane was incubated with protein-specific primary antibodies (Abcam) overnight. The following day, the membrane was probed with the corresponding secondary antibodies (Abcam) and NcmECL Ultra was used to develop the protein bands before the quantification of Keap1, Nrf2, and NQO1 protein expression.

Quantitative real-time PCR

Cells were cultured in a 6-well plate at a density of 1×10^6 cells/well for 24 h before treatment with CoNPs (400 μmol/l) with/or BNS (50 μg/ml) for a day at 37 °C, 5% CO₂. Total RNA was extracted from the cells using TRIzol reagent, following manufacturer's guidelines. The cDNA was transcribed from the RNA template using HiScript RT SuperMix (Vazyme, Nanjing, China), and then analyzed for the relative expressions of Nrf2 using AceQ qPCR SYBR Green Master Mix (Vazyme, Nanjing, China) and the MyiO2 Detection System (Bio-Rad Laboratories, Hercules, USA). The primer sequences used for the detection of Nrf2 were as follows: forward, 5'-ATG CCCTCACCTGCTACTTT-3' and reverse, 5'-AGG CCAAGTAGTGTGTCTCC-3'. The expression of each gene was normalized to the endogenous control β-actin, and was expressed, relative to the control, according to the $2^{-\Delta\Delta C_t}$ method.

Statistical analysis

All data were expressed as mean \pm SD (standard deviation) of three independent experiments performed in triplicates. Statistical analysis was performed using one-way analysis of variance (ANOVA), followed by the Dunnett's test. All statistical analyses were performed using SAS 9.4 statistical software (SAS Institute, Cary, NC, USA). A *p* value less than 0.05 was considered significant.

Results

Optimizing BNS concentration

The cells were incubated with CoNPs (400 μmol/l), along with differing concentrations of BNS, for 24 h, and the cell viability was assessed using the CCK-8 assay. As shown in Fig. 1B, low BNS concentrations, i.e., <45 μg/ml, were not able to protect the cells against ROS generation. Similarly, higher concentrations, i.e., >65 μg/ml, also did not have a protective effect on the CoNPs-exposed cells. Moreover, a concentration of 70 μg/ml BNS was found to be toxic for the cells, as evidenced by lower cell viability, as opposed to the CoNPs treatment alone. Based on our results, a BNS range of 45–60 μg/ml was shown to be optimal for preserving cell viability, even in the presence of CoNPs, relative to cells exposed to CoNPs alone.

BNS protects HUVECs from CoNPs toxicity

The average diameter of CoNPs used in this study was calculated as 30 nm via the TEM and SEM morphology (Liu et al. 2017). Cells were treated

with different concentrations of Co²⁺ and CoNPs for 24 h and the effect on HUVECs survival was determined by CCK-8 assay. The percentage of survived cells strikingly decreased with the increase of CoNPs concentration. In addition, the CoNPs showed higher toxicity than Co²⁺ at similar concentrations (Fig. 1A). There was around 50% reduction of viability of cells incubated with 400 μM of CoNPs for 24 h. Therefore, subsequent experiments were performed with 400 μM of CoNPs. Next, to quantify the toxicity levels of CoNPs (400 μmol/l) in HUVECs, the cells were exposed to CoNPs for 24, 48, and 72 h (Fig. 2) before measurement of cell viability, via the CCK-8 assay. As shown in Fig. 2A–C, the cell viability decreased over time by 49.96% ± 3.01%, 49.68% ± 2.44%, and 59.60% ± 2.73% (*p* < 0.05), respectively, as compared to cells without CoNPs. Alternately BNS addition antagonized the CoNPs-mediated cytotoxicity and improved cell viability by 37.40% ± 2.97%, 43.45% ± 1.93%, and 47.17% ± 2.41% at 24 h, 48 h, and 72 h, respectively (*p* < 0.05). Moreover, BNS addition alone did not produce any cytotoxicity and the cell viability observed in the BNS-exposed cells was slightly higher than cells that received no treatment.

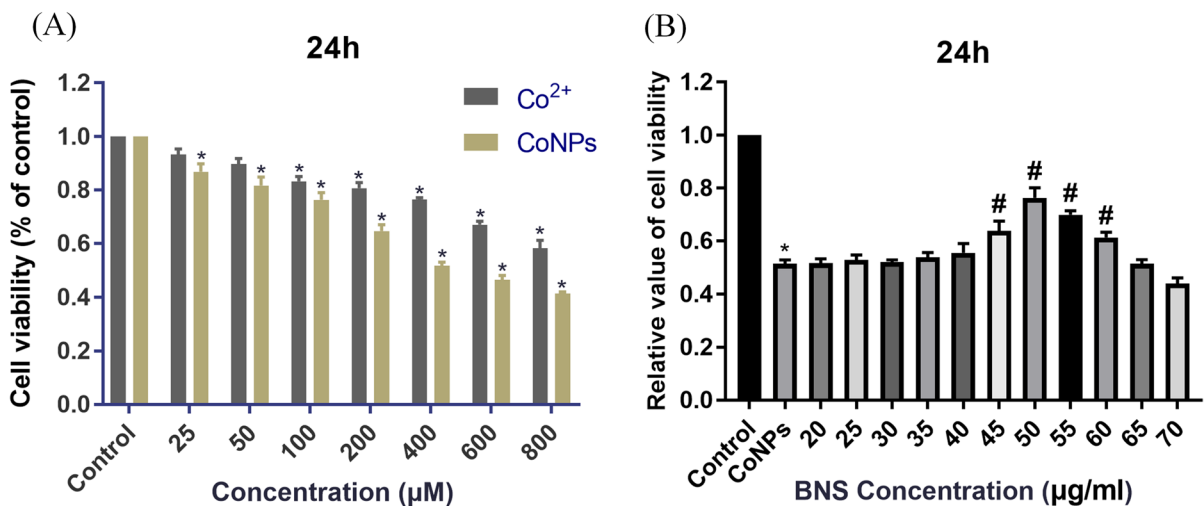


Fig. 1 Changes in cell viability of HUVECs following Co²⁺, CoNPs, and different concentrations of BNS for 24 h. (A) Viability of HUVECs exposed to 0–800 μM Co²⁺ and CoNPs for 24 h, as determined by a Cell Counting Kit-8 assay. (B) Effects of different concentrations of BNS on cell viability in

HUVECs when exposed to 400 μM CoNPs for 24 h. All data were expressed as mean ± SD of three independent experiments performed in triplicates. **p* < 0.05 compared with the control group. #*p* < 0.05 compared with the CoNPs group

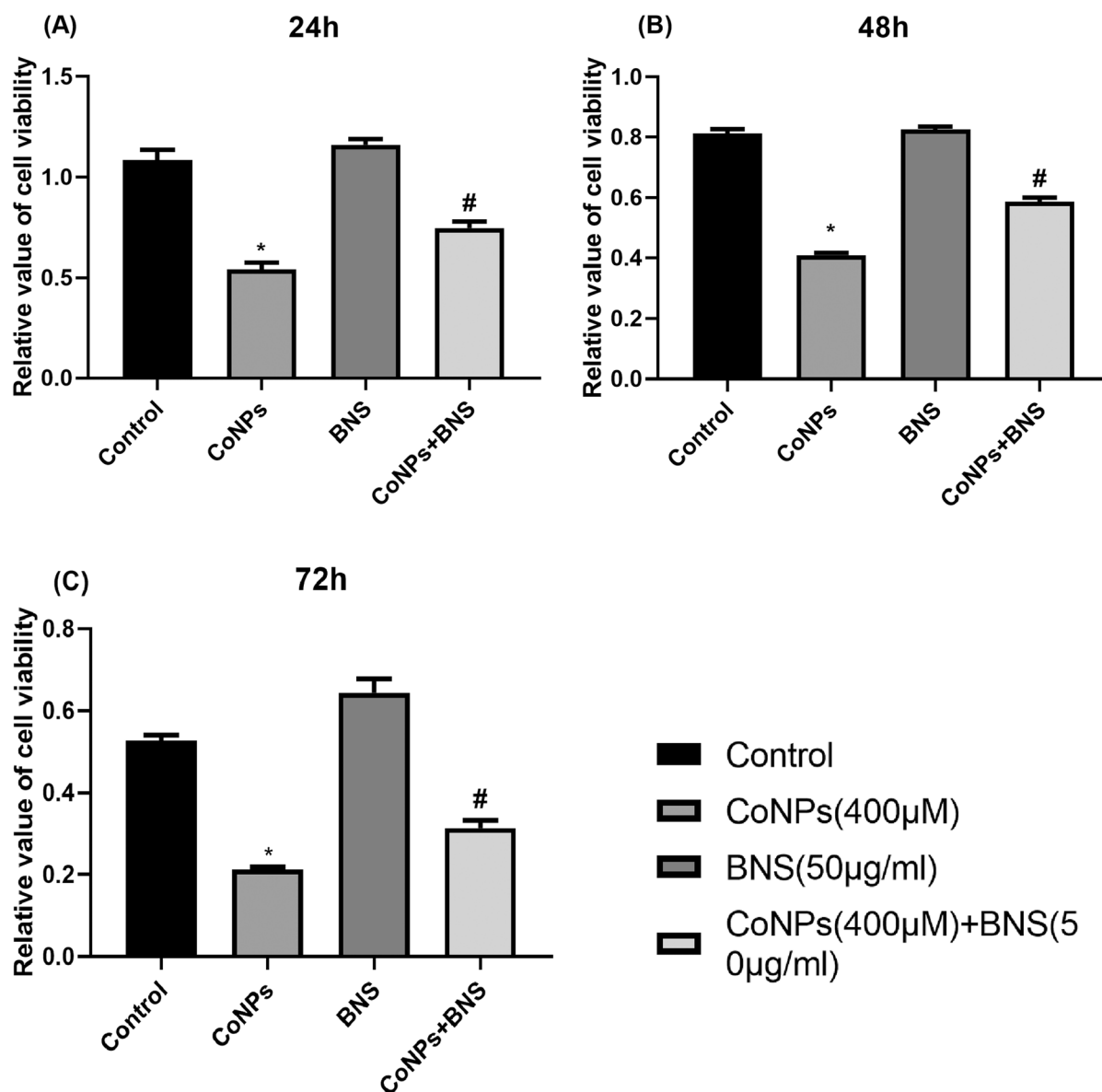


Fig. 2 The cell activity of HUVECs after exposure to CoNPs (400 μM) and BNS (50 μg/ml). Comparison of cell viability after exposure to CoNPs and BNS for 24 h, 48 h and 72 h, respectively. All data were expressed as mean ± SD of three

independent experiments performed in triplicates. * $p < 0.05$ compared with the control group. # $p < 0.05$ compared with the CoNPs group

BNS exposure suppressed inflammatory cytokines

As shown in Fig. 3, CoNPs exposure significantly upregulated the expression of cyto-inflammatory factors IL-1 β , IL-6, and TNF- α . Alternately, in cell receiving both CoNPs and BNS, the levels of IL-1 β , IL-6, and TNF- α reduced by 42.84% ± 2.16%,

51.05% ± 3.11%, and 43.22% ± 3.46%, respectively (Fig. 3A–C). Moreover, cells receiving BNS alone showed no obvious changes in inflammatory factors and no sign of cytotoxicity. Taken together, these results suggest that BNS suppresses the CoNPs-mediated activation of inflammatory factors in HUVECs.

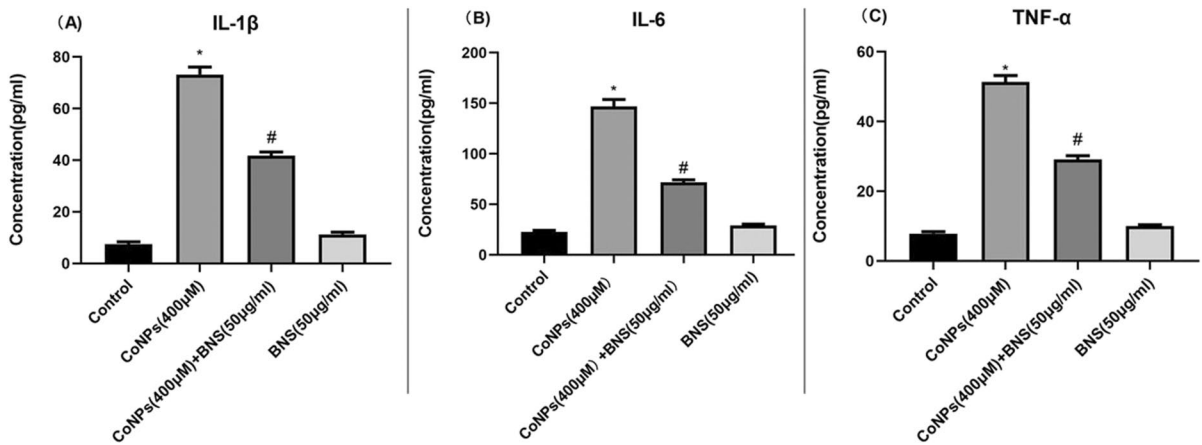


Fig. 3 BNS reduced the levels of IL-1β (A), IL-6 (B), and TNF-α (C) induced by CoNPs. Cells exposed to CoNPs (400 μM) and BNS (50 μg/ml) 24 h after the production of cytokine levels. All data were expressed as mean ± SD of three

independent experiments performed in triplicates. **p* < 0.05 compared with the control group. #*p* < 0.05 compared with the CoNPs group

BNS antagonizes CoNPs toxicity by activating the KNA signaling pathway

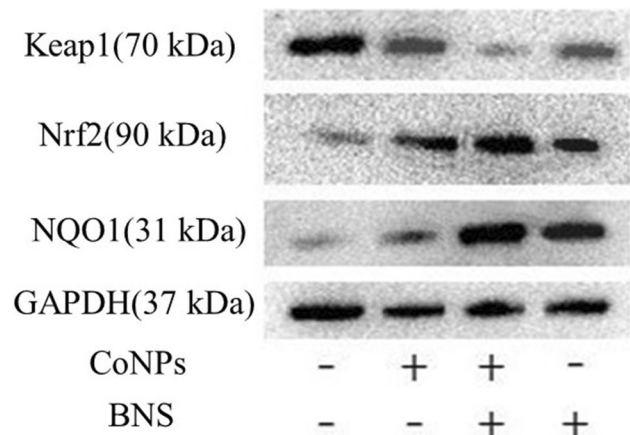
To characterize the underlying mechanism BNS employs to antagonize CoNPs-mediated cell toxicity, we analyzed the expression of the antioxidant signaling pathway KNA-related proteins and its downstream genes (Keap1, Nrf2, NQO1). As shown in Fig. 4 and Fig. 5, cells that received 400 μM CoNPs and 50 μg BNS for 24 h exhibited large increases in the protein Nrf2 and its downstream gene NQO1, as opposed to cells that received CoNPs alone. Based on our results, BNS activated the KNA pathway and its downstream antioxidant proteins to possibly protect

the cells against the damaging effects of CoNPs. Notably, we also discovered that CoNPs also activated the KNA pathway. However, this may be the cell’s own oxidative stress system gearing up to protect the cell from oxidative damage.

ROS formation

The fluorescence intensity of DCF produced by HUVECs treated with 400 μM CoNPs for 24 h was significantly higher than that of the control group, while the fluorescence intensity of DCF produced by HUVECs treated with 50 μg/ml BNS for 24 h was significantly lower than that of the control group, and

Fig. 4 The KNA pathway is involved in the process of BNS antagonizing the toxicity of CoNPs. After cells were exposed to CoNPs (400 μM) and BNS (50 μg) for 24 h, the expression of Keap1, Nrf2, and NQO1 was detected. Cells cultured with normal medium served as control group



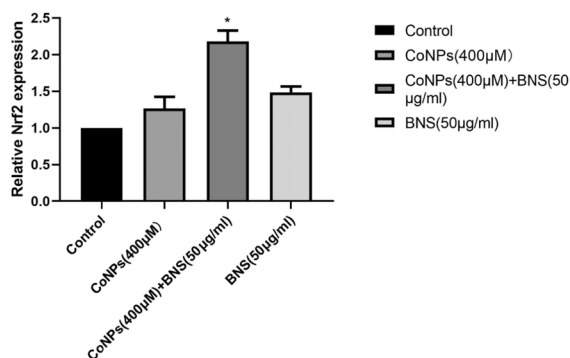


Fig. 5 RT-PCR was performed to detect mRNA expression levels of Nrf2. All data were expressed as mean \pm SD of three independent experiments performed in triplicates. * $p < 0.05$ compared with the control group. # $p < 0.05$ compared with the CoNPs group and control group

the difference was statistically significant (Fig. 6A, B). GSH is the key cellular endogenous antioxidant that can scavenge toxic free radicals, and depletion of GSH appears to promote intracellular ROS accumulation, leading to apoptosis. Altered GSH levels represent increased cellular response to oxidative stress. Our experimental results shows that CoNPs treatment decreased GSH levels ($p < 0.05$) and BNS reversed this decrease ($p < 0.05$) as measured by the GSH assay kit (Fig. 6C).

Discussion

Due to the massive integration of artificial joint replacements around the world, more and more artificial joint prostheses are implanted in the human body every day. Among the available prosthesis, the MOM prosthesis is the most popular due to its unique advantages (Kovochich et al. 2018). However, the MOM prosthesis is not without side effects. Once implanted in the body, nano-scale metal particles are released into the body due to various physical and chemical factors, inducing multiple health complications, including increased blood metal particle concentration, loosening of the prosthesis, pain, and early revision surgery (Law et al. 2020). Among the many metal particles potentially released by MOM prosthetics, CoNPs are the most toxic. However, not much is known about the underlying mechanism of cytotoxicity and genotoxicity caused by CoNPs (Trommer

and Maru 2016). One possible mechanism may involve the activation of the intracellular ROS system that produces a large number of ROS system products, thereby increasing intracellular oxidative and gene damage (Cappellini et al. 2018). Oxidative stress often activates the Keap1-Nrf2-ARE signaling pathway, a classic antioxidant pathway that stimulates the dissociation of Nrf2, from its complex with Keap1, so it can travel to the nucleus, where it combines with ARE to activate downstream genes (Bellezza et al. 2018). Due to its anti-oxidative property, KNA pathway is often upregulated when cells are challenged with CoNPs. This study demonstrated that BNS can be used to artificially upregulate the KNA pathway to counter the CoNPs-mediated cytotoxicity in HUVEC cells.

Our previous work suggested that the oxidative protection of BNS changes with differing concentrations. In other words, it only protects against toxicity at optimal concentrations. So, we first identified the optimal concentration of BNS that produces the maximal protection against CoNPs-mediated cell toxicity. We demonstrated that concentrations $< 45 \mu\text{g/ml}$ or $> 65 \mu\text{g/ml}$ yielded no protection against cytotoxicity. However, the range of $45\text{--}60 \mu\text{g/ml}$ BNS was ideal for cell viability, which remained high, as compared to the cells that received CoNPs alone. As a result, all subsequent experimentations involved a BNS concentration of $50 \mu\text{g/ml}$.

In this study, we used CCK-8 cell viability assay to analyze the rate of cell survival in cells exposed to CoNPs and BNS. The results showed that both CoNPs and Co^{2+} induced a decrease in the viability of HUVECs. The cytotoxic effects of CoNPs were stronger than Co^{2+} , which indicated that the CoNPs showed higher toxicity than Co^{2+} at similar concentrations. Based on our results, any level of CoNPs exposure significantly reduced cellular activity, indicating cytotoxicity. BNS administration, however, improved cell viability, even in the presence of toxic CoNPs. Our results were in accordance with others who reported a strong antioxidant property of BNS (Safdari-Rostamabad et al. 2017). Therefore, BNS was used in follow-up examinations to explore the underlying mechanism of cytotoxic protection in conditions of toxic exposure.

ROS is a collective name for a series of naturally occurring oxidative reactive products of oxygen metabolism. However, the presence of certain

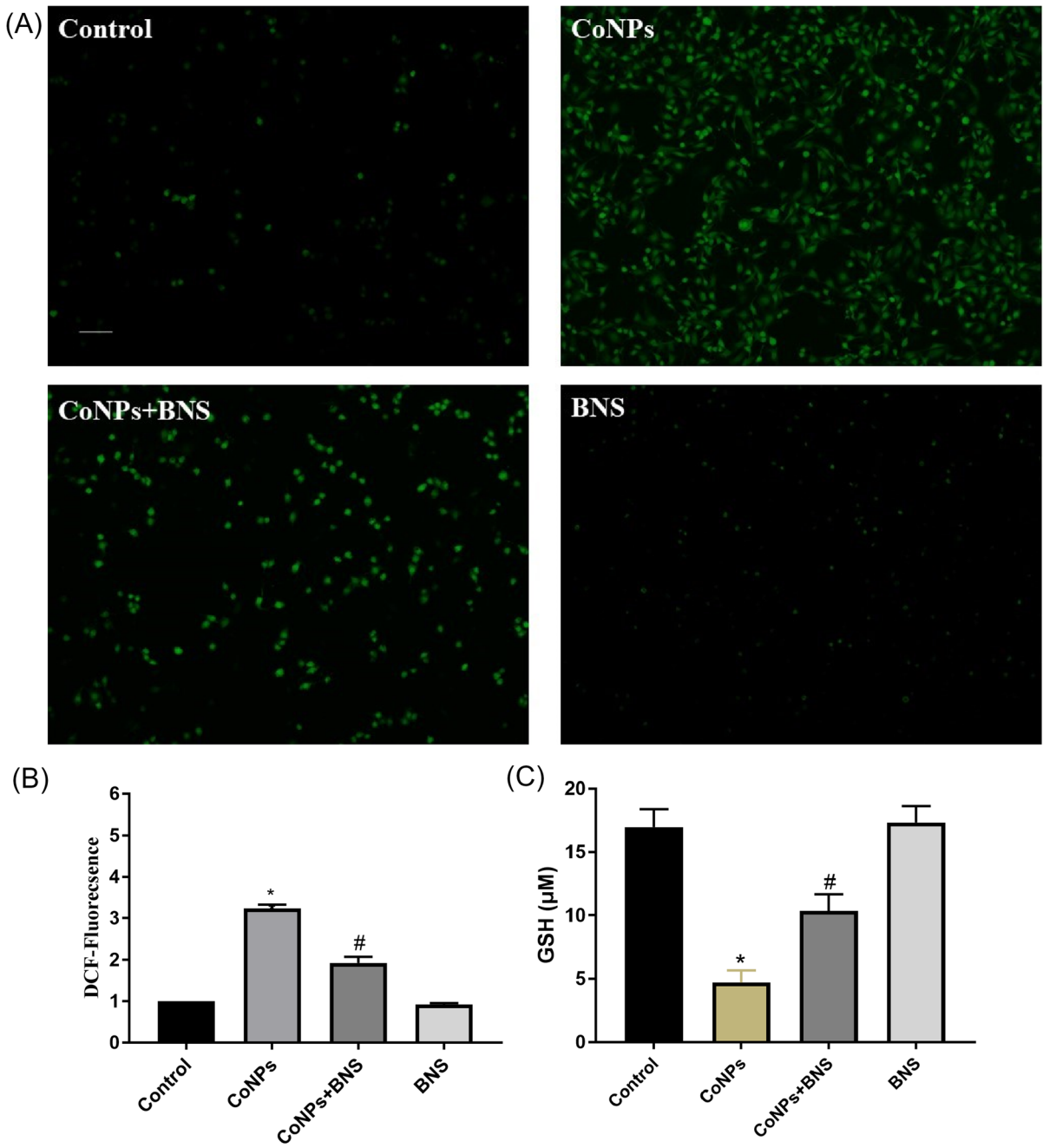


Fig. 6 Microphotographs showed generation of cellular ROS in HUVECs exposed to CoNPs and BNS (scale bar, 50 µm). Cells were exposed to 400 µM CoNPs with/without BNS for 24 h. (A) An upright fluorescence microscope was used to measure the intracellular fluorescence of cells. Each slide was scanned at $\times 100$. The green color indicates the fluorescence of

detected ROS production. (B) Relative percentage change in ROS generation was measured. (C) Effects of CoNPs on GSH in HUVECs. Cells were treated with CoNPs and BNS for 24 h. Each value represents the mean \pm SD of three independent experiments, performed in triplicates

factors like ultraviolet light and heat exposure sharply increases ROS generation, thereby incurring serious damage to cellular structure and function (Acker and Coenye 2017). For instance, ROS is known to oxidize DNA and induce breakage in DNA strands. Several studies have associated CoNPs with ROS production (Liu et al. 2015, 2016). Similar to other studies, our examinations also revealed that CoNPs-exposed cells had markedly increased ROS production and depletion of GSH, which is the key cellular endogenous antioxidant that can scavenge toxic free radicals, as opposed to untreated cells. Moreover, our results showed that the ROS production and depletion of GSH caused by CoNPs was partly attenuated by the addition of BNS.

Moreover, to characterize the BNS-mediated detoxification pathway, we examined the expression profile of inflammatory factors in CoNPs and/or BNS-exposed cells. Inflammatory factors are often upregulated under conditions of cellular damage and they drive the cell to apoptosis. Oxidative stress is one of the regulatory factors that induce an inflammatory response (Tian et al. 2017). Based on our results, CoNPs-exposed cells had remarkably high IL-1 β , IL-6, and TNF- α levels, which were partly abrogated in BNS-exposed cells. These results suggest that CoNPs induce oxidative stress in cells and BNS reduces cellular oxidative stress caused by CoNPs.

To further investigate the underlying mechanism of BNS cyto-protection, we explored the role of BNS in the regulation of a well-known antioxidant signaling pathway, KNA. KNA is regulated by cellular oxidative stress and functions by producing a series of antioxidant enzymes. In this study, we demonstrated that BNS administration upregulated the expression of Nrf2 and its downstream genes, suggesting that BNS activates KNA in order to attenuate oxidative stress, inflammation, cyto-, and possibly genotoxicity. Meanwhile, we also detected activation of the KNA pathway with CoNPs treatment alone. Since oxidative stress is one of the major regulators of the KNA pathway and one of the toxic responses of CoNPs is to elevate ROS production, it is possible that CoNPs activated KNA signaling through its upregulation of oxidative stress.

Our study highlights that CoNPs are highly toxic to HUVECs, and BNS can, in part, abrogate this toxicity. In the presence of BNS, the cells produced

less intracellular inflammatory factors and ROS system products. We also demonstrated that the KNA signaling pathway was employed by BNS in its abrogation of CoNPs cytotoxicity. Our research provides insight into the anti-toxic property of BNS and its underlying mechanism. The information provided in this study can benefit the development of new clinical therapeutics of CoNPs poisoning. Further in-depth study is warranted to determine the role of the KNA pathway in mediating the antioxidant and cytoprotective property of BNS and the specific way in which BNS activates KNA.

Conclusions

Our experiments confirmed that CoNPs have a clear toxic effect, and this effect is mainly achieved by increasing the production of ROS products. Based on this theory, we used BNS as an antidote to study its antagonistic effect and mechanism against the toxicity of CoNPs. The results showed that BNS reduced the inflammatory response and ROS production induced by CoNPs, which was related to the activation of KNA signaling pathway. The existing studies provide a theoretical basis for future in vivo experiments, and help to further study the relationship between KNA signaling pathway and BNS.

Abbreviations CoNPs: Cobalt nanoparticles; MOM: Metal-on-metal; ROS: Reactive oxygen species; KNA: Keap1-Nrf2-ARE; IARC: International Agency for Research on Cancer; HO-1: Heme oxygenase-1; NQO-1: Human quinone peroxidase-1; HUVECs: Human umbilical vein endothelial cells; FBS: Fetal bovine serum; PBS: Phosphate-buffered saline; CCTCC: China Center for Type Culture Collection; CCK-8: Cell Counting Kit-8; SD: Standard deviation

Acknowledgements The authors wish to thank Lei Yang (Tianjin Orthopaedic Research Institute, Tian Jing, China) for providing BNS.

Author contribution SW and CW researched literature and conceived the study. YL was involved in protocol development and data analysis. SW wrote the first draft of the manuscript. All authors reviewed and edited the manuscript and approved the final version of the manuscript.

Funding This work was supported by Postgraduate Research & Practice Innovation Program of Jiangsu Province [grant number SJCX20_1167].

Data availability The datasets used and/or analyzed during the current study are not publicly available. Data are however available from the corresponding author on reasonable request.

Declarations

Conflict of interest The authors declare that they have no conflict interest.

Open Access This article is licensed under a Creative Commons Attribution 4.0 International License, which permits use, sharing, adaptation, distribution and reproduction in any medium or format, as long as you give appropriate credit to the original author(s) and the source, provide a link to the Creative Commons licence, and indicate if changes were made. The images or other third party material in this article are included in the article's Creative Commons licence, unless indicated otherwise in a credit line to the material. If material is not included in the article's Creative Commons licence and your intended use is not permitted by statutory regulation or exceeds the permitted use, you will need to obtain permission directly from the copyright holder. To view a copy of this licence, visit <http://creativecommons.org/licenses/by/4.0/>.

References

- Alkhudhayri AA, Dkhal MA, Al-Quraishy S (2018) Nanosele-
nium prevents eimeriosis-induced inflammation and regu-
lates mucin gene expression in mice jejunum. *Int J Nano-
medicine* 3(13):1993–2003
- Bellezza I, Giambanco I, Minelli A, Donato R (2018) Nrf2-
Keap1 signaling in oxidative and reductive stress. *Bio-
chim Biophys Acta Mol Cell Res* 1865(5):721–733
- Cappellini F, Hedberg Y, McCarrick S et al (2018) Mechanistic
insight into reactivity and (geno)toxicity of well-charac-
terized nanoparticles of cobalt metal and oxides. *Nano-
toxicology* 12(6):602–620
- Han Q, Liu F (2017) Low doses of Co nanoparticles induce
death and regulate osteogenic differentiation in MG-63
cells. *Mol Med Rep* 16(5):7591–7596
- Kirkland D, Brock T, Haddouk H et al (2015) New investiga-
tions into the genotoxicity of cobalt compounds and their
impact on overall assessment of genotoxic risk. *Regul
Toxicol Pharmacol* 73(1):311–338
- Kovac S, Angelova PR, Holmström KM, Zhang Y, Dinkova-
Kostova AT, Abramov AY (2015) Nrf2 regulates ROS
production by mitochondria and NADPH oxidase. *Bio-
chim Biophys Acta* 1850(4):794–801
- Kovochich M, Finley BL, Novick R et al (2018) Understanding
outcomes and toxicological aspects of second generation
metal-on-metal hip implants: a state-of-the-art review. *Crit Rev Toxicol* 48(10):853–901
- Law JJ, Crawford DA, Adams JB, Lombardi AV Jr (2020)
Metal-on-metal total hip revisions: pearls and pitfalls. *J
Arthroplasty* 35(6S):S68–S72
- Learmonth ID, Young C, Rorabeck C (2007) The opera-
tion of the century: total hip replacement. *Lancet*
370(9597):1508–1519
- Leyssens L, Vinck B, Van Der Straeten C et al (2020) The
ototoxic potential of cobalt from metal-on-metal hip
implants: objective auditory and vestibular outcome. *Ear
Hear* 41(1):217–230
- Li M, Glassman A (2019) What's new in hip replacement. *J
Bone Joint Surg Am* 101(18):1619–1627
- Liu YK, Ye J, Han QL, Tao R, Liu F, Wang W (2015) Toxicity
and bioactivity of cobalt nanoparticles on the monocytes.
Orthop Surg 7(2):168–173
- Liu YK, Deng XX, Yang HL (2016) Cytotoxicity and geno-
toxicity in liver cells induced by cobalt nanoparticles and
ions. *Bone Joint Res* 5(10):461–469
- Liu Y, Hong H, Lu X et al (2017) L-ascorbic acid protected
against extrinsic and intrinsic apoptosis induced by cobalt
nanoparticles through ROS attenuation. *Biol Trace Elem
Res* 175:428–439
- Madl AK, Liang M, Kovochich M et al (2015) Toxicology of
wear particles of cobalt-chromium alloy metal-on-metal
hip implants Part I: physicochemical properties in patient
and simulator studies. *Nanomedicine* 11(5):1201–1215
- Miroliaee AE, Esmaily H, Vaziri-Bami A, Baeeri M, Shahverdi
AR, Abdollahi M (2011) Amelioration of experimental
colitis by a novel nanoselenium-silymarin mixture. *Toxi-
col Mech Methods* 21(3):200–208
- Packer M. (2016) Cobalt cardiomyopathy: a critical reap-
praisal in light of a recent resurgence. *Circ Heart Fail.*
2016;9(12):e003604.
- Perni S, Yang L, Preedy EC, Prokopovich P (2018) Cobalt and
Titanium nanoparticles influence on human osteoblast
mitochondrial activity and biophysical properties of their
cytoskeleton. *J Colloid Interface Sci* 531:410–420
- Polyzois I, Nikolopoulos D, Michos I et al (2012) Local and
systemic toxicity of nanoscale debris particles in total hip
arthroplasty. *J Appl Toxicol* 32(4):255–269
- Preedy EC, Perni S, Prokopovich P (2015) Cobalt, titanium and
PMMA bone cement debris influence on mouse osteoblast
cell elasticity, spring constant and calcium production
activity. *RSC Adv* 5(102):83885–83898
- Rasool A, Zulfajri M, Gulzar A, Hanafiah MM, Unnisa SA,
Mahboob M (2020) *Biotechnol Rep (Amst)*. 26:e00453
(Published 2020 Apr 20)
- Reich MS, Javidan P, Garg VK et al (2019) Chronic systemic
metal ion toxicity from wear on a revised cobalt-chrom-
ium trunnion. *J Orthop Case Rep* 9(2):48–51
- Safdari-Rostamabad M, Hosseini-Vashan SJ, Perai AH, Sarir
H (2017) Nanoselenium supplementation of heat-stressed
broilers: effects on performance, carcass characteris-
tics, blood metabolites, immune response, antioxidant
status, and jejunal morphology. *Biol Trace Elem Res*
178(1):105–116
- Saikko V (2019) Effect of wear, acetabular cup inclination
angle, load and serum degradation on the friction of a
large diameter metal-on-metal hip prosthesis. *Clin Bio-
mech (Bristol, Avon)* 63:1–9

- Song D, Cheng Y, Li X et al (2017) Biogenic nanoselenium particles effectively attenuate oxidative stress-induced intestinal epithelial barrier injury by activating the Nrf2 antioxidant pathway. *ACS Appl Mater Interfaces* 9(17):14724–14740
- Tian T, Wang Z, Zhang J (2017) Pathomechanisms of oxidative stress in inflammatory bowel disease and potential antioxidant therapies. *Oxid Med Cell Longev* 2017:4535194
- Trommer RM, Maru MM (2016) Importance of preclinical evaluation of wear in hip implant designs using simulator machines. *Rev Bras Ortop.* 52(3):251–259 (Published 2016 Dec 30)
- Van Acker H, Coenye T (2017) The role of reactive oxygen species in antibiotic-mediated killing of bacteria. *Trends Microbiol* 25(6):456–466
- Vera P, Canellas E, Nerín C (2018) New antioxidant multilayer packaging with nanoselenium to enhance the shelf-life of market food products. *Nanomaterials (Basel)* 8(10):837 (Published 2018 Oct 16)
- Wan R, Mo Y, Zhang Z, Jiang M, Tang S, Zhang Q (2017) Cobalt nanoparticles induce lung injury, DNA damage and mutations in mice. *Part Fibre Toxicol* 14(1):38 (Published 2017 Sep 18)
- Xiao X, Song D, Cheng Y et al (2019) Biogenic nanoselenium particles activate Nrf2-ARE pathway by phosphorylating p38, ERK1/2, and AKT on IPEC-J2 cells. *J Cell Physiol* 234(7):11227–11234
- Zhang XD, Zhao J, Bowman L, Shi X, Castranova V, Ding M (2010) Tungsten carbide-cobalt particles activate Nrf2 and its downstream target genes in JB6 cells possibly by ROS generation. *J Environ Pathol Toxicol Oncol* 29(1):31–40
- Zheng F, Luo Z, Zheng C et al (2019) Comparison of the neurotoxicity associated with cobalt nanoparticles and cobalt chloride in Wistar rats. *Toxicol Appl Pharmacol* 369:90–99
- Zorov DB, Juhaszova M, Sollott SJ (2014) Mitochondrial reactive oxygen species (ROS) and ROS-induced ROS release. *Physiol Rev* 94(3):909–950

Publisher's note Springer Nature remains neutral with regard to jurisdictional claims in published maps and institutional affiliations.